Novel derivatives of BCV and (S)-HPMPA inhibit orthopoxviruses and human adenoviruses more potently than BCV

Yifan Zhang[1,2,§], Yanmin Wan[1,3,#,§], Cuiyuan Guo[2,4,§], Zhaoqin Zhu[2,5,§], Chao Qiu[6,§], Jiasheng Lv[7,8,9], Yanan Zhou[10], Jiaojiao Zheng[5], Fahui Dai[5], Xiaoyang Cheng[1,2], Kunlu Deng[1,2], Wanhai Wang[3], Youchun Wang[9,11,#], Wenhong Zhang[1, #]

[1] Department of Infectious Diseases, Shanghai Key Laboratory of Infectious Diseases and Biosafety Emergency Response, National Medical Center for Infectious Diseases, Huashan Hospital, State Key Laboratory of Genetic Engineering, School of Life Science, Fudan University, China; Shanghai Sci-Tech Inno Center for Infection & Immunity, Shanghai 200052, China

[2] Department of laboratory medicine, Shanghai Public Health Clinical Center, Shanghai 201508, China

[3] Department of radiology, Shanghai Public Health Clinical Center, Shanghai 201508, China

[4] Clinical Laboratory, The First Affiliated Hospital of Zhengzhou University, Key Laboratory of Laboratory Medicine of Henan Province, Zhengzhou 450052, China

[5] Biosafety Level 3 Laboratory, Shanghai Public Health Clinical Center, Shanghai 201508, China

[6] Institutes of biomedical sciences & Shanghai Key Laboratory of Medical Epigenetics, Fudan University, Shanghai, China

[7] School of Life Sciences, Fudan University, Shanghai 200437, China

[8] Shenzhen Institutes of Advanced Technology, Chinese Academy of Sciences, Shenzhen 518055, China

[9] Risen (Shanghai) Pharma Tech Co., Ltd., Shanghai 201210, China

[10] Institute of Medical Biology, Chinese Academy of Medical Sciences and Peking Union Medical College, Kunming, China

[11] Key Laboratory of Pathogen Infection Prevention and Control (Peking Union Medical College), Ministry of Education, Beijing, China; State Key Laboratory of Respiratory Health and Multimorbidity, Beijing, China

[§] These authors contribute equally: Yifan Zhang, Yanmin Wan, Cuiyuan Guo, Zhaoqin Zhu and Chao Qiu

[#] These authors jointly supervised this work: Yanmin Wan, yanmin_wan@fudan.edu.cn; Youchun Wang, wangyc@nifdc.org.cn; Wenhong Zhang, zhangwenhong@fudan.edu.cn;

Running title: Novel prodrugs inhibit orthopoxviruses more potently than BCV

Word counts: main text, 4426 words; abstract, 231 words.

Abstract

BCV and tecovirimat are the only two chemical drugs that have been approved to treat smallpox and to treat Mpox under an FDA-authorized single-patient emergency use IND. Disappointedly, the efficacy of tecovirimat manifested in a recent clinical trial is far from being satisfactory, while the clinical efficacy of BCV is still inconclusive. Given that MPXV, variola and other emerging orthopoxviruses are posing serious threats to global health, it is urgent to develop new and better therapeutics. In this study, we tested the antiviral effects of three novel prodrugs, which were designed based on previously reported parent drugs, either (S)-HPMPC (cidofovir) or (S)-HPMPA. We found that one of the (S)-HPMPA-based prodrugs, ODE-(S)-HPMPA formate, exhibited significantly better anti-orthopoxvirus activity than BCV both in vitro and in vivo, which also inhibited human adenoviruses more efficiently than BCV. Most strikingly, the EC_{50} and EC_{90} of ODE-(S)-HPMPA formate against MPXV were more than 40-fold lower than those of BCV. In contrast, we observed that the anti-HSV-1 activities of the (S)-HPMPA-based prodrugs were less effective than those of the cidofovir-based prodrugs (BCV and BCV formate), especially in vivo. Moreover, we showed for the first time that cytidine and adenine analog combined therapies could provide mice complete protection against lethal challenges of both vaccinia and HSV-1. Collectively, we propose that both the ODE-(S)-HPMPA formate and the BCV/ODE-(S)-HPMPA formate combination are worth further investigations for their potential clinical applications.

Key words: Orthopoxvirus, HSV, Human adenovirus, Nucleos(t)ide analogue, BCV

Introduction

Viral polymerases are the most sought-after targets for developing anti-viral drugs [1-3]. Few dozens of viral RNA or DNA dependent polymerase inhibitors have been licensed for the treatment of human viral diseases, including brincidofovir (BCV, a prodrug of cidofovir), which is the second FDA approved drug for the treatment of smallpox infection [3, 4]. Given that variola and monkeypox virus (MPXV) are phylogenetically similar, the U.S. CDC suggests that BCV can be considered for the treatment of human Mpox disease in adults and pediatric patients under an FDA-authorized single-patient emergency use IND (e-IND).

BCV is a lipid conjugate of the nucleotide analogue cidofovir with broad-spectrum anti-double stranded DNA virus activity [5]. Data of previous studies suggested that the in vitro 50% inhibitory concentration (IC_{50}) of BCV against MPXV was relatively higher than that of tecovirimat [6-8], a specific inhibitor of orthopoxviruses targeting viral p37 protein orthologs [9]. Both compounds have been used to treat human Mpox disease [8, 10], but BCV can elevate the transaminases in the liver [11-13]. Tecovirimat has a relatively better safety profile [14] and is currently recommended by the U.S. CDC to be the first line treatment for MPXV infections in people. But at the same time, the U.S. CDC also alerts in the Guidance for Tecovirimat Use (https://www.cdc.gov/poxvirus/mpox/clinicians/Tecovirimat.html) that tecovirimat has a low barrier to viral resistance. A single amino acid mutation to the orthopoxviral p37 protein can lead to resistance to tecovirimat [15], which may be especially prong to occurrence among severely immunocompromised Mpox patients under multiple courses of tecovirimat treatment [16, 17]. Besides, according to data released from a clinical trial in the Democratic Republic of the Congo, tecovirimat neither accelerated recovery nor reduced mortality rate compared to placebo [18].

Mutations associated with cidofovir resistance have also been identified in multiple orthopoxviruses [8, 19] and human cytomegalovirus [20]. And mutations potentially associated with CDV resistance among the MPXVs of 2022 outbreak have been reported, too [8]. The prevalence of mutated MPXV may further rise once BCV was more widely and frequently used, which is also true for other orthopoxviruses because the mechanism of CDV resistance seems to be shared among the genus [21]. Given the

107 pacing threats posed by MPXV, variola and other emerging orthopoxviruses to human
108 health [22-25] , it is urgent to develop more safe and effective drugs.
109 CDV [(S)-1-(3-hydroxy-2-phosphonylmethoxypropyl)cytosine, HPMPC] and its prodrug
110 BCV exemplify that the (S)-HPMP nucleoside can be a promising class of broad
111 spectrum anti-viral compounds [5]. In fact, many others candidate molecules in this
112 class have been synthesized and tested for anti-viral effects. (S)-HPMPA [(S)-9-(3-
113 hydroxy-2-phosphonomethoxypropyl)-adenine] is one of these candidates, which
114 showed broad spectrum anti-viral activities in earlier studies [5, 26]. However, because
115 of the poor oral bioavailability, (S)-HPMPA is considered as not suitable for clinical use.
116 Great efforts have been made to modify (S)-HPMPA in order to increase their oral
117 bioavailabilities and anti-viral activities [27-35]. But only few candidate compounds, such
118 as ODE-(S)-HPMPA and HDP-(S)-HPMPA, displayed promising in vivo anti-
119 orthopoxvirus effects [30, 33]. In this work, we synthesized two novel (S)-HPMPA
120 prodrugs, ODE-(S)-HPMPA formate and HDP-(S)-HPMPA formate, and a new CDV
121 prodrug, BCV formate, and tested their anti-viral effects in parallel with BCV both in vitro
122 and in vivo.
123
124 **Materials and methods**
125 **Ethical Statement**
126 Experiments using mice were approved by the Research Ethics Review Committee of
127 the Shanghai Public Health Clinical Center Affiliated to Fudan University. Experiments
128 using live vaccinia, HSV-1 and adenoviruses were conducted in a BSL-2 or ABSL-2 lab.
129 Measurements of in vitro inhibition of MPXV were performed in a BSL-3 lab.
130 **Antiviral compounds**
131 BCV (CAS number 444805-28-1, purity 99.82%) was purchased from Shanghai
132 Haohong Scientific Co., Ltd.. Three candidate compounds were synthesized by our
133 collaborator, Risen (Shanghai) Pharma Tech Co., Ltd. Compound BCV formate (purity
134 97.86%) is a derivative of cidofovir. Compound ODE-(s)-HPMPA formate (purity 95.03%)
135 and compound HDP-(s)-HPMPA formate (purity 96.97%) are prodrugs of (S)-HPMPA.
136 The molecular formulas of these compounds and their active metabolites are shown in
137 Figure1.

138 **Virus propagation and titration**

139 Vaccinia Tiantan strain was propagated in Vero cells. Briefly, confluent Vero cells plated
140 in 100mm×10mm petri dishes were inoculated with Tiantan vaccinia at a multiplicity of
141 infection (MOI) of 0.01. After 2 hours absorption at 37°C with 5% CO_2, the inoculum was
142 removed and 10ml of fresh maintenance medium (DMEM containing 3% FBS and 1%
143 PS) was added to each dish. The cell cultures were maintained at 37°C with 5% CO_2 for
144 another 2 days. After that, propagated vaccinia viruses were harvested by three rapid
145 freeze-thaw cycles of the infected cells. HSV-1 propagation followed a similar protocol
146 except that the inoculum was adsorbed for 1 hour with gentle agitation at room
147 temperature and the propagated virus was harvested from the culture supernatant by
148 centrifuging at 34,000g for 2 hours at 4°C [36]. MPXV was sourced from National
149 Kunming High-level Biosafety Primate Research Center, Institute of Medical Biology,
150 Chinese Academy of Medical Sciences and Peking Union Medical College. Viruses
151 were amplified in Vero cells, cultured in DMEM supplemented with 2% FBS and 1% PS.
152 Harvested vaccinia, MPXV and HSV-1 viruses were titrated using plaque assays. Briefly,
153 confluent monolayers of Vero cells in 24-well plates were infected with 10-fold serial
154 dilutions of each virus, ranging from 10^{-1} to 10^{-9}. For vaccinia viruses and MPXV, the
155 plates were incubated at 37°C with 5% CO_2 for 2 hours. For HSV-1 (strain-17), the
156 plates were gently agitated at room temperature for 1 hour. After absorption, the cells
157 were overlaid with 800 μL of overlay medium (DMEM containing 1% FBS and 1.25%
158 methyl cellulose) and incubated at 37°C with 5% CO_2 for 4 days. Post-incubation, the
159 plates were fixed with 4% neutral formalin and stained with crystal violet. Plaques were
160 visually counted, and the viral titers were calculated and expressed as plaque-forming
161 units (PFU) per milliliter.

162 HAdV-B21 and C2 were isolated from nasopharyngeal swab specimens of HAdV-
163 positive patients and propagated in HEp-2 cells. Briefly, HEp-2 cells were plated in
164 100mm×10mm petri dishes and inoculated with hAdVs. After a 1-hour adsorption at 37°
165 C with 5% CO_2, the inoculum was removed, and 10 mL of maintenance medium was
166 added to each dish. The cultures were maintained at 37°C with 5% CO_2 until more than
167 80% of the cells exhibited cytopathic effects (CPE). Propagated hAdVs were harvested
168 by three rapid freeze-thaw cycles of the infected cells.

169 The stocks of hAdVs were titrated using the $TCID_{50}$ assay. Briefly, confluent monolayers
170 of Vero cells in 96-well cell culture plates were infected with 10-fold serial dilutions of
171 the hAdVs. The wells were monitored for the presence of CPE and the infectious
172 adenovirus titer was determined as $TCID_{50}$ per mL using the Spearman-Karber method.

173 **Cytotoxicity assays**

174 The cytotoxicities of candidate compounds were determined using a Promega CellTiter-
175 Glo® Luminescent Cell Viability Assay kit (Cat#G7571, Madison, WI, USA) according to
176 the manufacturer's instructions. Briefly, Vero cells were seeded in 96-well plates and
177 incubated overnight. Then, cells were exposed to either the solvent control (DCM:MeOH,
178 v:v=1:3) or diluted candidate compounds. Each concentration was tested in
179 quadruplicate. The plates were incubated for 72 hours at 37°C with 5% CO_2.
180 Subsequently, reconstituted Steady-Glo reagent was added and assay plates were
181 incubated for 10 min at room temperature. The luminescence was measured using a
182 luminescence microplate reader (GloMax® Navigator Microplate Luminometer,
183 Promega, USA). Wells containing culture medium without cells served as blank controls.
184 Cell viabilities were calculated using the following equation: Cell viability (%) = (drug
185 treated well - blank) / (solvent treated well - blank) × 100%.

186 **In vitro viral inhibition assays**

187 20 PFU of orthopoxvirus (Tiantan vaccinia or MPXV) or HSV-1 virus suspended in 200
188 μL maintenance medium were transferred onto confluent Vero cell monolayers in 24-
189 well plates. For vaccinia virus, the plates were incubated at 37°C with 5% CO_2 for 2
190 hours. For HSV-1, the plates were gently agitated at room temperature for 1 hour. 800
191 μL of overlay-medium containing DCM:MeOH (v:v=1:3) or serially diluted candidate
192 compounds was added to each well after removing the inoculums. The plates were then
193 incubated for 4 days at 37°C with 5% CO_2. Finally, the plates were fixed with 4% neutral
194 formalin and stained with crystal violet. The number of plaques in each well was visually
195 counted. All compounds were tested in quadruplicates at each dilution. The viral
196 inhibition rate was calculated using the formula: Inhibition rate (%) = (1 − the average
197 plaque number of the sample wells / the average plaque number of the solvent wells) ×
198 100%.

199 In vitro inhibition of hAdV B21 and C2 were performed as described previously [37].
200 Briefly, 25,000 Vero cells were plated in each well of a 96-well cell culture plate,
201 followed by addition of diluted adenovirus (with 50 and 200 $TCID_{50}$/well for B21 and C2,
202 respectively) and serially diluted candidate compounds. The solvent was used as the
203 non-treated control. The plates were then incubated at 37°C with 5% CO_2 for 4 days.
204 Cytopathology was quantitively assessed using a Promega CellTiter-Glo® Luminescent
205 Cell Viability Assay kit. The viral inhibition rate was calculated using the formula:
206 inhibition rate (%) = (drug treated well – blank) - (non-treated control well – blank) ×
207 100%.

208 **In vivo evaluation of anti-viral effects**

209 We established mouse infection models to evaluate the anti-viral effects of the
210 candidate compounds against Tiantan vaccinia and HSV-1, respectively. 6×10^6 PFU of
211 Vaccinia virus (Tiantan strain) suspended in 40 μL 1×PBS was instilled intranasally into
212 4-week-old male BALB/c mice under transient anesthesia of inhaled isoflurane (Cat#
213 R510-22, Ryward RWD). For HSV-1 infections, 4-week-old female BALB/c mice were
214 infected intraperitoneally with 1×10^8 PFU of HSV-1 suspended in 200 μL of 1×PBS.
215 After infection, mice were weighed daily to monitor disease progression and mice that
216 lost ≥30% of their initial body weight were deemed ethically dead. All mice were daily
217 monitored to the end of the experiment and biological death cause by vaccinia infection
218 were also recorded. For treatment experiments, mice were given equal moles of
219 candidate compounds dissolved in saline containing 5% DMSO, 10% Solutol, and 17%
220 SBE-β-CD via oral gavage at days 1, 3 and 5 post-infection as specified in Figure 4-6.
221 Control animals received an equivalent volume of the vehicle via the same gavage
222 method. Infected mice were euthanized at timepoints indicated in Figure 4-6. Samples
223 of multiple organs were collected for viral titration, host response assay or
224 pharmaceutical analysis.

225 **Pharmaceutical analyses of mouse tissue samples**

226 Anticoagulated mouse blood samples were collected and centrifuged at 3200 rpm for 10
227 minutes at 4°C to separate the plasma, which was then aliquoted and stored at -80°C
228 until analysis. Tissue samples, including spleen, brain, liver, kidney, lung, and testes,
229 were homogenized and centrifuged at 4100g for 15 minutes to obtain supernatants for

230 pharmacokinetic analysis. The concentrations of the candidate compounds,
231 intermediate metabolites, and active metabolites in both plasma and tissue samples
232 were determined using a validated liquid chromatography-tandem mass spectrometry
233 (LC-MS/MS) method, as described in the literature [38]. The lower limits of quantitation
234 (LLOQ) were 1 ng/mL in plasma, and in tissues, the LLOQs were 10 ng/g for ODE-(s)-
235 HPMPA and BCV, 20 ng/g for CDV, and 50 ng/g for HPMPA and HDP-(s)-HPMPA.

236 **Titration of Tiantan vaccinia and HSV-1 in mouse organs**

237 Tissue samples were pre-cooled on ice and homogenized using high-throughput tissue
238 grinding machine (Cat# Scientz-192, NingBo Scientz Biotechnology Co., Ningbo City,
239 China). After that, the homogenates were centrifuged at 2000g for 10 minutes and the
240 supernatants were collected for viral titration following similar procedures to those
241 described above for in vitro viral titration. Briefly, confluent monolayers of Vero cells in
242 24-well plates were inoculated with 10-fold serially diluted supernatants of tissue
243 homogenates. After incubation, the wells were overlaid with 800 μL of overlay medium
244 and incubated for 4 days. Finally, the plates were fixed with neutral formalin and stained
245 with crystal violet, and plaques were counted to determine viral titers.

246 **Histological examination**

247 Tissue samples of multiple mouse organs were collected at 7 days post Tiantan
248 vaccinia infection. Collected tissues were fixed in 4% neutral paraformaldehyde for 2
249 hours, followed by standard processing and embedding in paraffin. Tissue sections
250 were stained with hematoxylin and eosin (H&E). The stained slides were analyzed using
251 the KF-PRO-120 digital pathology slide scanner (KFBIO) to assess tissue morphology
252 and the extent of pathological changes. The images were analyzed and exported by K-
253 VIEWER1.5.5.6 software.

254 **Detection of cytokine transcription in mouse lung**

255 Total RNA was extracted from mouse lung tissues collected at multiple timepoints post
256 Tiantan vaccinia infection using Trizol reagent (Cat# 15596026CN, Life Technologies).
257 1 μg of total RNA from each sample was reversely transcribed using the HiScript II Q
258 RT SuperMix for qPCR (+gDNA wiper) (R223-01, Vazyme, China). Real-time PCR was
259 conducted with the TB Green® Premix Ex Taq™ II (Tli RNase H Plus) (Cat# RR820Q,
260 TaKaRa) using an ABI 7500 real-time fluorescence quantitative PCR (qPCR) instrument

261 (Thermo Fisher Technology Co., LTD., Shanghai, China). Transcription levels of
262 cytokine genes relative to the GAPDH gene were calculated using the $2^{-\Delta Ct}$ method,
263 where ΔCt = Ct of the target gene - Ct of GAPDH. The primers of mouse cytokines and
264 GAPDH genes used for qRT-PCR are listed in Supplemental table 1, which were
265 synthesized according to a previous work [39].

266 **Determination of Alanine Aminotransferase (ALT) in murine serum**

267 Peripheral blood was collected from mice at 2 days post the third dose of drug treatment.
268 Serum was separated after clotting at room temperature for 1 hour by centrifuging at
269 1000g for 10 minutes at 4°C. Serum ALT activity was determined using a
270 commercialized ELISA kit following the manufacturer's protocol (Cat# JL12668, Jianglai
271 Biotechnology, Shanghai, China). Optical density was measured at 450 nm using a
272 microplate reader (Cat# 800TS, Biotek, USA).

273 **Statistical methods**

274 Statistical analyses were conducted using GraphPad Prism 9 (GraphPad Software,
275 USA). The normality of the data was checked before all downstream statistical analyses.
276 Comparisons between two groups were performed by the method of t-test. Differences
277 among multiple groups were compared by the method of one-way ANOVA. EC_{50} and
278 EC_{90} values were calculated using a four-parameter variable slope non-linear
279 regression method. Survival curves were compared by the Cox-Mantel test. $P \leq 0.05$
280 was considered as statistically significant.

281

282 **Results**

283 **In vitro cytotoxicity and in vivo pharmacokinetics of candidate compounds**

284 Synthesized compounds (BCV formate, ODE-(s)-HPMPA formate and HDP-(s)-HPMPA
285 formate) were dissolved in DCM:MeOH (v:v=1:3) at a maximum concentration of 10μM.
286 Cytotoxicity assays showed that all compounds were well tolerated at concentrations of
287 5μM and 10μM in Vero cells (Figure 2A and 2B).
288 To facilitate in vivo antiviral activity evaluation, we monitored the kinetics of absorption
289 and metabolism for each compound after a single dose of oral gavage in mice. Our data
290 showed that all compounds or their metabolites were detectable at a half hour post oral
291 intake (Figure 2C and 2D), suggesting that they could be quickly assimilated into blood.

292 After absorption, BCV formate, ODE-(s)-HPMPA formate and HDP-(s)-HPMPA formate
293 were instantly hydrolyzed into BCV, ODE-(s)-HPMPA and HDP-(s)-HPMPA,
294 respectively. And the concentrations of these metabolites in blood peaked around 1 to 2
295 hours post intake (Figure 2C and 2D). Then, BCV was gradually hydrolyzed into CDV
296 within 24 hours post oral intake (Figure 2E). While ODE-(s)-HPMPA and HDP-(s)-
297 HPMPA were hydrolyzed faster into HPMPA, which lasted only 8 hours (Figure 2F).
298 **ODE-(s)-HPMPA formate and HDP-(s)-HPMPA formate showed superior anti-**
299 **orthopoxvirus activities than BCV and BCV formate**
300 To compare the anti-orthopoxvirus effects of the candidate drugs with BCV, we firstly
301 tested their antiviral activities against vaccinia Tiantan strain and MPXV in vitro. Our
302 data showed that the EC_{50} and EC_{90} of BCV formate against Tiantan vaccinia were
303 similar with those of BCV, while the EC_{50} and EC_{90} of ODE-(s)-HPMPA formate and
304 HDP-(s)-HPMPA formate were conspicuously lower (Figure 3A). Notably, ODE-(s)-
305 HPMPA formate displayed the lowest EC_{50} and EC_{90}, which were around 15-fold lower
306 than BCV (Figure 3A). The anti-MPXV activity of BCV was similar with its effect against
307 Tiantan vaccinia, while the other three compounds inhibited MPXV even more actively
308 than Tiantan vaccinia (Figure 3B). ODE-(s)-HPMPA formate demonstrated the most
309 potent anti-MPXV effect, whose EC_{50} and EC_{90} were more than 40-fold lower than those
310 of BCV (Figure 3B).
311 Next, we evaluated the in vivo anti-orthopoxvirus activities of the synthesized
312 compounds using a lethal mouse model of vaccinia virus infection. As shown in Figure
313 4A, 4 weeks old BALB/c mice were intra nasally infected with 6×10^6 pfu of vaccinia
314 Tiantan strain. Equal moles of candidate drugs were given at 1 day, 3 days and 5 days
315 post infection via oral gavage. All groups of infected mice experienced obvious body
316 weight loss, which peaked around 7 to 8 days post infection for mice treated with BCV
317 formate, ODE-(s)-HPMPA formate or HDP-(s)-HPMPA formate (Figure 4B). In contrast,
318 mice received the vehicle or BCV underwent more severe weight loss and all mice in
319 these two groups ethically died by day 8 (Figure 4B). Over 90% of mice (10 out of 11)
320 treated with ODE-(s)-HPMPA formate survived, which was significantly better than mice
321 received vehicle, BCV or BCV formate (Figure 4C). The second-best drug was HDP-(s)-
322 HPMPA formate, which protected significantly more mice from death than vehicle and

323 BCV (Figure 4C). BCV formate also displayed better protection, but its efficacy did not
324 significantly differ from those of the vehicle and BCV (Figure 4C).
325 To characterize the in vivo anti-vaccinia virus activities further, we repeated vaccinia
326 virus infection and drug treatment in mice, but this time 3-5 mice of each group were
327 euthanized at each indicated time points for detections of viral replication, host
328 responses and drug metabolites (Figure 5A). We found that vaccinia virus resided
329 mainly in lungs after intra nasal infection and significant suppression of the virus by
330 candidate drugs could be observed in all detected tissues except kidney (Figure 5B-5G),
331 where live vaccinia viruses were rarely detected even in the non-treated group.
332 Compared to BCV, BCV formate, ODE-(s)-HPMPA formate and HDP-(s)-HPMPA
333 formate tended to decrease vaccinia virus titers in lungs, but statistical significance was
334 only observed between BCV and ODE-(s)-HPMPA formate at day 3 and between BCV
335 and HDP-(s)-HPMPA formate at day 5 (Figure 5B). Histopathology examination showed
336 that ODE-(s)-HPMPA formate and HDP-(s)-HPMPA formate diminished the size of lung
337 lesions caused by vaccinia infection compared to BCV and BCV formate at 7 days post
338 infection (Figure 5H). Meanwhile, no signs of infection-caused or drug-related pathology
339 were observed in other organs, including the kidney, spleen, testis, liver and brain
340 (Supplementary figure 1). We also monitored the cytokine responses in lungs at 3, 5, 7,
341 10 and 14 days post infection. We found that different drugs impacted lung inflammation
342 differentially (Supplementary figure 2). Of note, at 7 days post vaccinia infection
343 (approximately the nadir of mouse body weight change), the transcription levels of IL-6
344 in lungs of mice treated with ODE-(s)-HPMPA formate were significantly lower than
345 those of mice treated with vehicle or BCV (Supplementary figure 2A). While, the levels
346 of IL-12 and TNF-a transcripts in lungs of mice treated with ODE-(s)-HPMPA formate or
347 BCV formate were significantly higher than those of mice treated with vehicle or BCV
348 (Supplementary figure 2B and 2C). These findings were partially in accordance with a
349 previous study suggesting that HPMPA could activate TNF-a secretion [40].
350 We noticed that livers contained the highest concentrations of drug metabolites during
351 the whole process of drug treatments (Supplementary figure 3). Hence, we assessed
352 the liver toxicities of candidate drugs via measuring the serum ALT levels at day 7 (2
353 days post the third dose of drug treatment). The results showed that the average levels

354 of plasma ALT ranked as follows: HDP-(s)-HPMPA formate > BCV formate > BCV >
355 vehicle > ODE-(s)-HPMPA formate > uninfected control (Supplementary figure 4). Of
356 note, the ALT levels of BCV, BCV formate and HDP-(s)-HPMPA formate treated mice
357 were significantly higher than uninfected controls, while no significant difference was
358 observed among ODE-(s)-HPMPA formate, vehicle and control groups (Supplementary
359 figure 4).

360 **ODE-(s)-HPMPA formate and HDP-(s)-HPMPA formate could suppress HSV-1 both**
361 **in vivo and in vitro, but were less effective than BCV and BCV formate in**
362 **protecting mice against lethal infection**

363 As NAs usually have broad spectrum antiviral activity [41], we next compared the anti-
364 HSV-1 activities between the candidate drugs and BCV. The results of in vitro antiviral
365 assays indicated that the EC_{50} and EC_{90} of BCV formate and ODE-(s)-HPMPA formate
366 against HSV-1 were close to those of BCV, while the EC_{50} and EC_{90} of HDP-(s)-HPMPA
367 formate were slightly higher (Figure 6A). To validate this observation, we tested their
368 efficacies against HSV-1 lethal infection in vivo. As shown in Figure 6B, BALB/c mice
369 were intra peritoneally infected with 1×10^8 pfu of HSV-1 (strain-17) followed by the
370 same regimen of drug treatment with vaccinia infected mice. Our data showed that BCV
371 and BCV formate alleviated mouse body weight loss, whereas ODE-(s)-HPMPA formate
372 and HDP-(s)-HPMPA formate apparently did not (Figure 6C). Albeit ODE-(s)-HPMPA
373 formate and HDP-(s)-HPMPA formate provided significant protection against lethal
374 HSV-1 infection than the vehicle, their protection rates were significantly lower than
375 those of BCV and BCV formate (Figure 6D). It is intriguing to see that the adenine
376 analogs (ODE-(s)-HPMPA formate and HDP-(s)-HPMPA formate) were more effective
377 in protecting mice against vaccinia infection while less effective towards HSV-1 infection
378 compared to cytidine analogs (BCV and BCV formate). We further compared the
379 genomic DNA base composition of orthopoxvirus with that of HSV and found that
380 orthopoxviruses contain obviously less GC than HSV (Supplementary figure 5 and
381 Supplementary table 2). This difference might lead to that adenine analogs would have
382 more chance to be incorporated into orthopoxvirus genome, while the cytidine analogs
383 would be more frequently incorporated into HSV genome.

384 Inspired by this observation, we were curious whether a combined regimen of purine
385 and pyrimidine analogs would provide more balanced protection against orthopoxvirus
386 and herpesvirus. To test this hypothesis, we treated vaccinia infected mice with the
387 equal molar mixture of BCV formate and ODE-(s)-HPMPA formate, and treated HSV-1
388 infected mice with the equal molar mixture of BCV formate and ODE-(s)-HPMPA
389 formate (Supplementary figure 6A). The total dosage for each mixed regimen was
390 maintained in consistency with the aforementioned single-drug regimen. The result
391 showed that all mice survived after being treated with the combined regimens
392 (Supplementary figure 6B), which was obviously better than any single-drug treatment
393 shown in Figure 4 and Figure 6.

394 **Three candidate compounds exhibited relatively better in vitro anti-hAdV activity**
395 **than BCV**

396 BCV has been used compassionately to treat adenovirus infection for pediatric patients
397 receiving hematopoietic stem cell transplantation [42]. In this study, we compared the
398 anti-hAdV potencies between three candidate prodrugs and BCV using clinically
399 isolated strains of hAdV type C2 and type B21. Generally, the EC_{50} values of the three
400 candidates, especially those of BCV formate and ODE-(s)-HPMPA formate, were much
401 lower than the EC_{50} values BCV (Figure 7). Considering that the liver toxicity of ODE-
402 (s)-HPMPA formate were significantly lower than BCV formate (Supplementary figure 4),
403 we thought ODE-(s)-HPMPA formate could also be good candidate therapeutic for
404 hAdV infections.

405

406 **Discussion**

407 Nucleoside/nucleotide analogues (NAs) have been widely used to treat cancer and viral
408 diseases [43]. Given that the catalytic units of viral polymerases are conserved in their
409 structures [44], NAs are thought to be an important class of broad-spectrum antiviral
410 agents [41]. Since the first anti-viral NA was approved in 1969, more than two dozen of
411 NAs have been licensed to treat viral infections [45]. However, only limited number of
412 viral diseases are targeted [3]. Among the six families of double stranded DNA viruses
413 (Hepadnaviridae, Polyomaviridae, Papillomaviridae, Adenoviridae, Herpesviridae
414 and Poxviridae) known to cause human diseases [46], only five viruses from three

415 families (Hepadnaviridae, Herpesviridae and Poxviridae) can be treated with approved
416 NAs [3, 4]. BCV is currently the only NA that can be used to treat human Mpox disease
417 under an FDA-authorized single-patient e-IND, while its efficacy is still inconclusive [47].
418 Bottlenecks, such as toxicity, poor oral bioavailability and limited translatability, restrain
419 NAs from being applied to more viral diseases [41, 45]. In this work, we and
420 collaborators synthesized a new precursor of CDV and two novel precursors of (S)-
421 HPMPA and evaluated their inhibitory activities against multiple double-stranded DNA
422 viruses, including orthopoxviruses, HSV-1 (strain 17) and human adenoviruses.
423 Through the experiments shown here, we found that BCV and three candidate prodrugs
424 exhibited varied antiviral potencies against different DNA viruses. The anti-
425 orthopoxvirus potency of BCV formate was non-inferior to BCV, by contrast the two
426 prodrugs of (S)-HPMPA were remarkably more effective than BCV in suppressing
427 orthopoxviruses both in vitro and in vivo. ODE-(s)-HPMPA formate was the best-
428 performing anti-orthopoxvirus compound, which displayed the most robust anti-
429 orthopoxvirus activity and the lowest hepatotoxicity. ODE-(s)-HPMPA formate and HDP-
430 (s)-HPMPA formate were designed based on previously reported ODE-(s)-HPMPA and
431 HDP-(s)-HPMPA [30, 33]. We did not test the latter compounds in parallel in this study,
432 but compared to the published data [33], both ODE-(s)-HPMPA formate and HDP-(s)-
433 HPMPA formate are much more efficacious than their counterparts in protecting mice
434 from lethal vaccinia infection (Supplementary table 3).
435 A second key finding of this work is that BCV and BCV formate provided significantly
436 stronger protection against lethal HSV-1 infection than ODE-(s)-HPMPA formate and
437 HDP-(s)-HPMPA formate in mice. The primary anti-viral mechanism of NAs is that they
438 resemble natural nucleos(t)ides and act by being incorporated into the nascent DNA
439 chain [48, 49], however the mechanism underlying the varied protective effects against
440 orthopoxvirus and HSV-1 is not clear. As herpesvirus genome contains obviously more
441 GC than orthopoxvirus genome, we speculate that the cytidine analogs (BCV and BCV
442 formate) might be more effective in suppressing herpesviruses, while adenine analogs,
443 ODE-(s)-HPMPA formate and HDP-(s)-HPMPA formate, might inhibit orthopoxviruses
444 more efficiently. Consistent with this hypothesis, we proved that combined regimens of
445 cytidine and adenine analogs could provide excellent protection against both vaccinia

446 and HSV-1 infection in mice, indicating that combination of purine and pyrimidine
447 analogs might be a rational and promising strategy to develop a broad-spectrum
448 antiviral therapy.
449 Finally, we tested the anti-hAdV potencies of the candidate prodrugs through in vitro
450 experiments. Adenoviruses can cause life-threatening disease not only in
451 immunocompromised patients but also in the healthy, although the latter occurs less
452 frequently [50, 51]. Both CDV and BCV have been compassionately used to treat hAdV
453 infections in children receiving hematopoietic cell transplantation [42, 52], but there are
454 no officially approved therapeutics. Here we showed ODE-(s)-HPMPA formate could be
455 a good anti-hAdV agent, which exhibited a good safety profile and relatively stronger
456 inhibitory effect than BCV.
457 A major limitation of this work is that we did not test the in vivo anti-MPXV and anti-
458 hAdV effects of the candidate prodrugs, primarily because no appropriate animal
459 models are available to us. Evaluations using an MPXV infected rhesus macaque model
460 [53] and an hAdV infected human lung organoid model [54] may provide more relevant
461 data before moving any of the candidate prodrugs into clinical trials.
462

463 **Declaration of competing interests**

464 Patent applications regarding the novel prodrugs evaluated in this study have been
465 jointly filed by Shanghai Sci-Tech Inno Center for Infection & Immunity and Risen
466 (Shanghai) Pharma Tech Co., Ltd.. The authors declare no other competing interests.
467

468 **Author contributions**

469 Yanmin Wan, Wenhong Zhang and Youchun Wang jointly supervised the study. Yanmin
470 Wan, Zhaoqin Zhu and Chao Qiu designed the experiments. Yanmin Wan, Yifan Zhang,
471 Cuiyuan Guo, Jiasheng Lv, Yanan Zhou, Jiaojiao Zheng, Fahui Dai, Xiaoyang Cheng
472 and Kunlu Deng conducted the experiments. Yanmin Wan, Yifan Zhang and Cuiyuan
473 Guo analyzed the data and drafted the manuscript. Yanmin Wan, Zhaoqin Zhu and
474 Wanhai Wang revised the manuscript. All authors approved the submitted version.
475

476 **Acknowledgments**

We thank Quanlin Xue from Fudan University for kindly sharing HSV-1 (strain 17) with us. This work was supported in part by the National Natural Science Foundation of China (Grant No. 32270986), the major project of Study on Pathogenesis and Epidemic Prevention Technology System by the Ministry of Science and Technology of China (Grant No. 2021YFC2302500) and the National Key Research and Development Program of China (Grant No. 2022YFC2009802).

References

1. Lu, L., et al., *Antivirals with common targets against highly pathogenic viruses.* Cell, 2021. **184**(6): p. 1604-1620.
2. Peng, S., et al., *Progression of Antiviral Agents Targeting Viral Polymerases.* Molecules, 2022. **27**(21).
3. Palazzotti, D., et al., *Small Molecule Drugs Targeting Viral Polymerases.* Pharmaceuticals (Basel), 2024. **17**(5).
4. Chan-Tack, K., et al., *Benefit-risk assessment for brincidofovir for the treatment of smallpox: U.S. Food and Drug Administration's Evaluation.* Antiviral Res, 2021. **195**: p. 105182.
5. Magee, W.C. and D.H. Evans, *The antiviral activity and mechanism of action of (S)-[3-hydroxy-2-(phosphonomethoxy)propyl] (HPMP) nucleosides.* Antiviral Res, 2012. **96**(2): p. 169-80.
6. Bojkova, D., et al., *Drug Sensitivity of Currently Circulating Mpox Viruses.* N Engl J Med, 2023. **388**(3): p. 279-281.
7. Frenois-Veyrat, G., et al., *Tecovirimat is effective against human monkeypox virus in vitro at nanomolar concentrations.* Nat Microbiol, 2022. **7**(12): p. 1951-1955.
8. Byrareddy, S.N., et al., *Potential therapeutic targets for Mpox: the evidence to date.* Expert Opin Ther Targets, 2023. **27**(6): p. 419-431.
9. Duraffour, S., G. Andrei, and R. Snoeck, *Tecovirimat, a p37 envelope protein inhibitor for the treatment of smallpox infection.* IDrugs, 2010. **13**(3): p. 181-91.
10. Shamim, M.A., et al., *The use of antivirals in the treatment of human monkeypox outbreaks: a systematic review.* Int J Infect Dis, 2023. **127**: p. 150-161.
11. Adler, H., et al., *Clinical features and management of human monkeypox: a retrospective observational study in the UK.* Lancet Infect Dis, 2022. **22**(8): p. 1153-1162.
12. Barnes, A.H., et al., *Mpox: Special Considerations in the Immunocompromised Host.* Current Treatment Options in Infectious Diseases, 2022. **14**(4): p. 43-66.
13. Imran, M., et al., *Oral Brincidofovir Therapy for Monkeypox Outbreak: A Focused Review on the Therapeutic Potential, Clinical Studies, Patent Literature, and Prospects.* Biomedicines, 2023. **11**(2).
14. Grosenbach, D.W., et al., *Oral Tecovirimat for the Treatment of Smallpox.* N Engl J Med, 2018. **379**(1): p. 44-53.
15. Duraffour, S., et al., *ST-246 is a key antiviral to inhibit the viral F13L phospholipase, one of the essential proteins for orthopoxvirus wrapping.* J Antimicrob Chemother, 2015. **70**(5): p. 1367-80.
16. Smith, T.G., et al., *Tecovirimat Resistance in Mpox Patients, United States, 2022-2023.* Emerg Infect Dis, 2023. **29**(12): p. 2426-2432.

17. Alarcón, J., et al., *An Mpox-Related Death in the United States.* N Engl J Med, 2023. **388**(13): p. 1246-1247.
18. Lenharo, M., *Hopes dashed for drug aimed at monkeypox virus spreading in Africa.* Nature, 2024. **632**(8027): p. 965.
19. Andrei, G. and R. Snoeck, *Cidofovir Activity against Poxvirus Infections.* Viruses, 2010. **2**(12): p. 2803-30.
20. Lurain, N.S. and S. Chou, *Antiviral drug resistance of human cytomegalovirus.* Clin Microbiol Rev, 2010. **23**(4): p. 689-712.
21. Farlow, J., et al., *Comparative whole genome sequence analysis of wild-type and cidofovir-resistant monkeypoxvirus.* Virol J, 2010. **7**: p. 110.
22. Silva, N.I.O., et al., *Here, There, and Everywhere: The Wide Host Range and Geographic Distribution of Zoonotic Orthopoxviruses.* Viruses, 2020. **13**(1).
23. Zhang, Y., et al., *Potential threat of human pathogenic orthopoxviruses to public health and control strategies.* J Biosaf Biosecur, 2023. **5**(1): p. 1-7.
24. Shchelkunov, S.N., *An increasing danger of zoonotic orthopoxvirus infections.* PLoS Pathog, 2013. **9**(12): p. e1003756.
25. Shchelkunova, G.A. and S.N. Shchelkunov, *Smallpox, Monkeypox and Other Human Orthopoxvirus Infections.* Viruses, 2022. **15**(1).
26. De Clercq, E. and A. Holý, *Acyclic nucleoside phosphonates: a key class of antiviral drugs.* Nat Rev Drug Discov, 2005. **4**(11): p. 928-40.
27. Tollefson, A.E., et al., *Oral USC-093, a novel homoserinamide analogue of the tyrosinamide (S)-HPMPA prodrug USC-087 has decreased nephrotoxicity while maintaining antiviral efficacy against human adenovirus infection of Syrian hamsters.* Antiviral Res, 2024. **222**: p. 105799.
28. Luo, M., et al., *Amidate Prodrugs of Cyclic 9-(S)-[3-Hydroxy-2-(phosphonomethoxy)propyl]adenine with Potent Anti-Herpesvirus Activity.* ACS Med Chem Lett, 2018. **9**(4): p. 381-385.
29. Beadle, J.R., *Synthesis of cidofovir and (S)-HPMPA ether lipid prodrugs.* Curr Protoc Nucleic Acid Chem, 2007. **Chapter 15**: p. Unit 15.2.
30. Quenelle, D.C., et al., *Effect of oral treatment with (S)-HPMPA, HDP-(S)-HPMPA or ODE-(S)-HPMPA on replication of murine cytomegalovirus (MCMV) or human cytomegalovirus (HCMV) in animal models.* Antiviral Res, 2008. **79**(2): p. 133-5.
31. Dal Pozzo, F., et al., *In vitro evaluation of the anti-orf virus activity of alkoxyalkyl esters of CDV, cCDV and (S)-HPMPA.* Antiviral Res, 2007. **75**(1): p. 52-7.
32. Morrey, J.D., et al., *Alkoxyalkyl esters of 9-(s)-(3-hydroxy-2-phosphonomethoxypropyl) adenine are potent and selective inhibitors of hepatitis B virus (HBV) replication in vitro and in HBV transgenic mice in vivo.* Antimicrob Agents Chemother, 2009. **53**(7): p. 2865-70.
33. Quenelle, D.C., et al., *Effect of oral treatment with hexadecyloxypropyl-[(S)-9-(3-hydroxy-2- phosphonylmethoxypropyl)adenine] [(S)-HPMPA] or octadecyloxyethyl-(S)-HPMPA on cowpox or vaccinia virus infections in mice.* Antimicrob Agents Chemother, 2007. **51**(11): p. 3940-7.
34. Beadle, J.R., et al., *Synthesis and antiviral evaluation of alkoxyalkyl derivatives of 9-(S)-(3-hydroxy-2-phosphonomethoxypropyl)adenine against cytomegalovirus and orthopoxviruses.* J Med Chem, 2006. **49**(6): p. 2010-5.
35. Ruiz, J., et al., *Synthesis, metabolic stability and antiviral evaluation of various alkoxyalkyl esters of cidofovir and 9-(S)-[3-hydroxy-2-(phosphonomethoxy)propyl]adenine.* Bioorg Med Chem, 2011. **19**(9): p. 2950-8.

36. Grosche, L., et al., *Herpes Simplex Virus Type 1 Propagation, Titration and Single-step Growth Curves.* Bio Protoc, 2019. **9**(23): p. e3441.
37. Hartline, C.B., et al., *A standardized approach to the evaluation of antivirals against DNA viruses: Orthopox-, adeno-, and herpesviruses.* Antiviral Res, 2018. **159**: p. 104-112.
38. Painter, W., et al., *First pharmacokinetic and safety study in humans of the novel lipid antiviral conjugate CMX001, a broad-spectrum oral drug active against double-stranded DNA viruses.* Antimicrob Agents Chemother, 2012. **56**(5): p. 2726-34.
39. Wang, X., et al., *Immune Correlates of Disseminated BCG Infection in IL12RB1-Deficient Mice.* Vaccines (Basel), 2022. **10**(7).
40. Potmesil, P., et al., *Nucleotide analogues with immunobiological properties: 9-[2-Hydroxy-3-(phosphonomethoxy)propyl]-adenine (HPMPA), -2,6-diaminopurine (HPMPDAP), and their N6-substituted derivatives.* Eur J Pharmacol, 2006. **540**(1-3): p. 191-9.
41. Karim, M., C.W. Lo, and S. Einav, *Preparing for the next viral threat with broad-spectrum antivirals.* J Clin Invest, 2023. **133**(11).
42. Perruccio, K., et al., *Safety and efficacy of brincidofovir for Adenovirus infection in children receiving allogeneic stem cell transplantation: an AIEOP retrospective analyses.* Bone Marrow Transplant, 2021. **56**(12): p. 3104-3107.
43. Jordheim, L.P., et al., *Advances in the development of nucleoside and nucleotide analogues for cancer and viral diseases.* Nature Reviews Drug Discovery, 2013. **12**(6): p. 447-464.
44. Peersen, O.B., *A Comprehensive Superposition of Viral Polymerase Structures.* Viruses, 2019. **11**(8).
45. Jordheim, L.P., et al., *Advances in the development of nucleoside and nucleotide analogues for cancer and viral diseases.* Nat Rev Drug Discov, 2013. **12**(6): p. 447-64.
46. Modrow, S., et al., *Viruses with a Double-Stranded DNA Genome*, in *Molecular Virology*, S. Modrow, et al., Editors. 2013, Springer Berlin Heidelberg: Berlin, Heidelberg. p. 625-873.
47. Li, P., et al., *Clinical Features, Antiviral Treatment, and Patient Outcomes: A Systematic Review and Comparative Analysis of the Previous and the 2022 Mpox Outbreaks.* J Infect Dis, 2023. **228**(4): p. 391-401.
48. *Nucleoside Analogues*, in *LiverTox: Clinical and Research Information on Drug-Induced Liver Injury*. 2012, National Institute of Diabetes and Digestive and Kidney Diseases: Bethesda (MD).
49. Kamzeeva, P.N., et al., *Recent Advances in Molecular Mechanisms of Nucleoside Antivirals.* Curr Issues Mol Biol, 2023. **45**(8): p. 6851-6879.
50. Khanal, S., P. Ghimire, and A.S. Dhamoon, *The Repertoire of Adenovirus in Human Disease: The Innocuous to the Deadly.* Biomedicines, 2018. **6**(1).
51. Dotan, M., et al., *Adenovirus can be a serious, life-threatening disease, even in previously healthy children.* Acta Paediatr, 2022. **111**(3): p. 614-619.
52. Hiwarkar, P., et al., *Brincidofovir is highly efficacious in controlling adenoviremia in pediatric recipients of hematopoietic cell transplant.* Blood, 2017. **129**(14): p. 2033-2037.
53. Aid, M., et al., *Mpox infection protects against re-challenge in rhesus macaques.* Cell, 2023. **186**(21): p. 4652-4661.e13.
54. Zhao, S., et al., *Generation of Human Embryonic Stem Cell-Derived Lung Organoids for Modeling Infection and Replication Differences between Human Adenovirus Types 3 and 55 and Evaluating Potential Antiviral Drugs.* J Virol, 2023. **97**(5): p. e0020923.

618 **Figure Legends**

619 **Figure 1 Illustration of the molecular formulae and the theoretical metabolic**
620 **pathways of BCV and the newly synthesized prodrugs**

621 After two steps of hydrolysis, BCV formate can be converted to the same active parent
622 drug (CDV) with BCV. ODE-(s)-HPMPA formate and HDP-(s)-HPMPA formate also take
623 two steps of hydrolysis to turn into HPMPA.

624

625 **Figure 2 In vitro cytotoxicity and in vivo pharmacokinetic analyses of BCV and**
626 **the candidate compounds**

627 (**A-B**) Comparisons of cytotoxicities between candidate compounds and BCV. Limited
628 by the solubility of BCV formate, ODE-(s)-HPMPA formate and HDP-(s)-HPMPA
629 formate, the highest concentration employed in the cytotoxicity assay was 10μM. All
630 compounds were tested in quadruplicated wells and the solvent was used as the
631 negative control to calculate the percentage of cell viabilities. Data are presented as
632 mean ± SD. (**C-D**) Plasma concentrations of BCV, BCV formate, ODE-(s)-HPMPA
633 formate and HDP-(s)-HPMPA formate, as well as their respective one-step hydrolytic
634 metabolites CDV, BCV, ODE-(s)-HPMPA and HDP-(s)-HPMPA, were measured at
635 various time points following a single oral gavage dose (3 mice per group). (**E-F**)
636 Plasma concentrations of BCV, ODE-(s)-HPMPA, and HDP-(s)-HPMPA, as well as their
637 hydrolytic metabolites (CDV and HPMPA) were measured at various time points
638 following a single oral gavage dose (3 mice per group).

639

640 **Figure 3 In vitro evaluations of anti-vaccinia and anti-MPXV activities of BCV and**
641 **the candidate compounds**

642 Vero cells were infected with vaccinia Tiantan strain (**A**) or MPXV (**B**) and treated with
643 the indicated concentrations of BCV or the candidate prodrugs. All compounds were
644 tested in triplicated wells at each concentration. The solvent was used as the non-
645 treated control. The antiviral effects were determined by calculating the reduction in
646 plaque formation. Data are presented as mean ± SD.

647

648 **Figure 4 ODE-(s)-HPMPA formate and HDP-(s)-HPMPA formate showed superior**
649 **therapeutic efficacies against lethal Tiantan vaccinia infection in mice**
650 (**A**) The schematic illustration of experimental design. (**B-C**) Weight loss and survival
651 rates of mice after being intra nasally infected with the vaccinia Tiantan strain. Mice
652 received the solvent served as the non-treated control. Weight loss ≥30% of initial body
653 weight was recorded as ethical death and was therefore not represented in the figure.
654 The data of weight loss are presented as mean ± SD. Mice that lost ≥30% of their initial
655 body weight were deemed ethically dead. Statistical significance is indicated as follows:
656 *, $, #: $p < 0.05$; **, $$, ##: $p < 0.01$; ***, $$$, ###: $p < 0.001$; ****, $$$$, ####: $p <$
657 0.0001.
658
659 **Figure 5 ODE-(s)-HPMPA formate and HDP-(s)-HPMPA formate more effectively**
660 **reduced lung vaccinia virus titers and mitigated pathological severity compared**
661 **to BCV and BCV formate**
662 (**A**) The schematic illustration of experimental design. (**B-G**) Viral titers in the lung,
663 spleen, kidney, brain, testis, and liver were measured by plaque assays at 3, 5, 7, 10,
664 and 14 days post-infection, respectively. (**H**) Histopathological examination of lung
665 tissue at 7 days post infection. Black outlines indicate areas of observed pathology, and
666 the percentages of the lesion area relative to the total area of the tissue are denoted in
667 red.
668
669 **Figure 6 Evaluations of in vivo and in vitro anti-HSV-1 potencies of BCV and the**
670 **candidate prodrugs**
671 (**A**) Vero cells were infected with HSV-1 stain 17 and treated with indicated
672 concentrations of BCV or the candidate compounds. All compounds were tested in
673 triplicated wells at each concentration. The solvent was used as the non-treated control.
674 The antiviral effects were determined by calculating the reduction in plaque formation.
675 Data are presented as mean ± SD. (**B**) The schematic illustration of in vivo experiment
676 design. (**C-D**) Weight loss and survival rates of mice after being intra
677 peritoneally infected with HSV-1. Mice received the solvent served as the non-treated
678 control. The data of weight loss are presented as mean ± SD. Weight loss ≥30% of initial

679 body weight was recorded as ethical death and was therefore not represented in the
680 figure. Statistical significance is indicated as follows: *, $, #: $p < 0.05$; **, $$, ##: $p <$
681 0.01; ***, $$$, ###: $p < 0.001$; ****, $$$$, ####: $p < 0.0001$.
682
683 **Figure 7 In vitro evaluation of anti-hAdV activities of BCV and the candidate**
684 **compounds**
685 Vero cells were infected with either hAdV C2 (**A**) or hAdV B21 (**B**) and subsequently
686 treated with indicated concentrations of BCV or the candidate prodrugs. All compounds
687 were tested in quadruplicate at each concentration. The solvent was used as the non-
688 treated control. Data are presented as mean ± SD.
689
690
691
692
693
694
695
696
697
698

699 **Supplementary figure legends**

700 **Supplementary figure 1 No signs of infection-caused and drug-related pathology**

701 Histopathological examination of the kidneys, spleen, testis, liver, and brain in mice at 7
702 days post Tiantan vaccinia infection.

703

704 **Supplementary figure 2 Drug treatment impacted pulmonary cytokine responses**
705 **in mice following intranasal infection with Tiantan vaccinia**

706 The transcriptional levels of IL-6 (**A**), IL-12 (**B**), TNF-α (**C**), IL-2 (**D**), IL-1β (**E**), IFN-γ (**F**),
707 IL-4 (**G**) in lung tissues were assessed at 3, 5, 7, 10, and 14 days post-infection with the
708 Tiantan vaccinia virus.

709

710 **Supplementary figure 3 Monitoring in vivo drug metabolites throughout the**
711 **treatment course**

712 (**A-D**) The concentrations of drug metabolites in mouse plasma, lung, kidney, spleen
713 and liver were measured using HPLC-MS at 3, 5, 7, 10 and 14 days post infection,
714 respectively (3 mice per group). Metabolites of all drugs were non-detectable in the
715 brain and testis at any time point. Data are presented as mean ± SD.

716

717 **Supplementary figure 4 Detection of ALT levels in mouse serum**

718 Serum ALT levels were measured at 2 days after the third dose drug treatment (n=5).
719 Data are presented as mean ± SD.

720

721 **Supplementary figure 5 Comparison of genome GC content between Tiantan**
722 **vaccinia and HSV-1**

723 A representative Tiantan vaccinia genome sequence (accession number: KC207811.1)
724 and a representative HSV-1 genome sequence (accession number: X14112.1) were
725 retrieved from GenBank. The GC content was analyzed using a sliding window
726 approach in the Biostrings package of R package, with a window size of 1000 base
727 pairs.

728

729 **Supplementary figure 6 Adenine and cytidine analog combinations showed**
730 **complete protection against both vaccinia and HSV-1 infections**
731 (**A**) The schematic illustration of experimental design. (**B**) Weight loss of mice after
732 being infected with Tiantan vaccinia or HSV-1. Data are presented as mean ± SD.

Figure 1

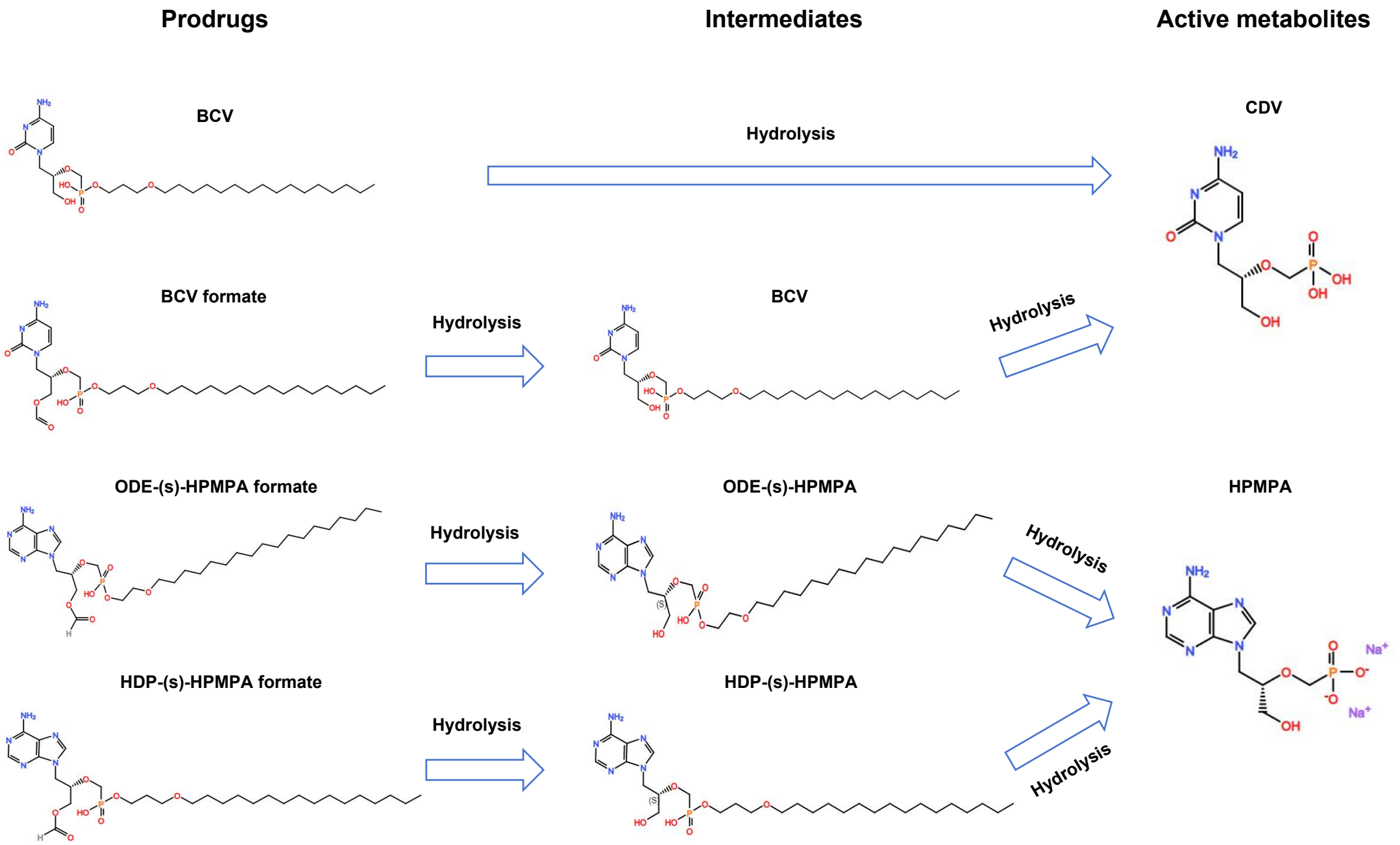
Prodrugs
Intermediates
Active metabolites
BCV
Hydrolysis
CDV
BCV formate
Hydrolysis
BCV
Hydrolysis
ODE-(s)-HPMPA formate
ODE-(s)-HPMPA
HPMPA
Hydrolysis
Hydrolysis
HDP-(s)-HPMPA formate
HDP-(s)-HPMPA
Hydrolysis
Hydrolysis

Figure 2

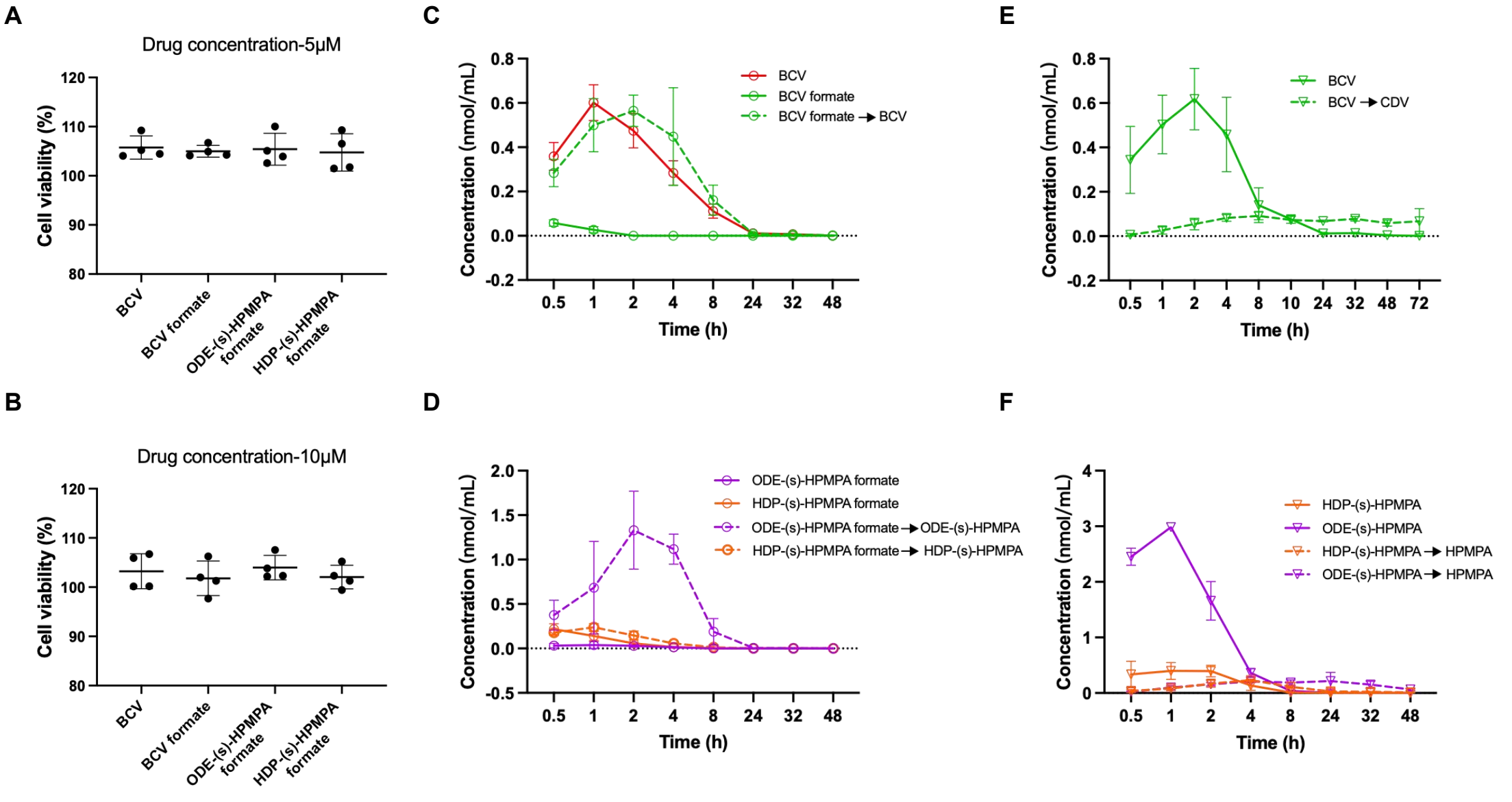
A
Drug concentration-5μM
Cell viability (%)
120
110
100
90
80
BCV
BCV formate
ODE-(s)-HPMPA formate
HDP-(s)-HPMPA formate
B
Drug concentration-10μM
Cell viability (%)
120
110
100
90
80
BCV
BCV formate
ODE-(s)-HPMPA formate
HDP-(s)-HPMPA formate
C
Concentration (nmol/mL)
0.8
0.6
0.4
0.2
0.0
-0.2
0.5
1
2
4
8
24
32
48
Time (h)
BCV
BCV formate
BCV formate → BCV
D
Concentration (nmol/mL)
2.0
1.5
1.0
0.5
0.0
-0.5
0.5
1
2
4
8
24
32
48
Time (h)
ODE-(s)-HPMPA formate
HDP-(s)-HPMPA formate
ODE-(s)-HPMPA formate → ODE-(s)-HPMPA
HDP-(s)-HPMPA formate → HDP-(s)-HPMPA
E
Concentration (nmol/mL)
0.8
0.6
0.4
0.2
0.0
-0.2
0.5
1
2
4
8
10
24
32
48
72
Time (h)
BCV
BCV → CDV
F
Concentration (nmol/mL)
4
3
2
1
0
0.5
1
2
4
8
24
32
48
Time (h)
HDP-(s)-HPMPA
ODE-(s)-HPMPA
HDP-(s)-HPMPA → HPMPA
ODE-(s)-HPMPA → HPMPA

Figure 3

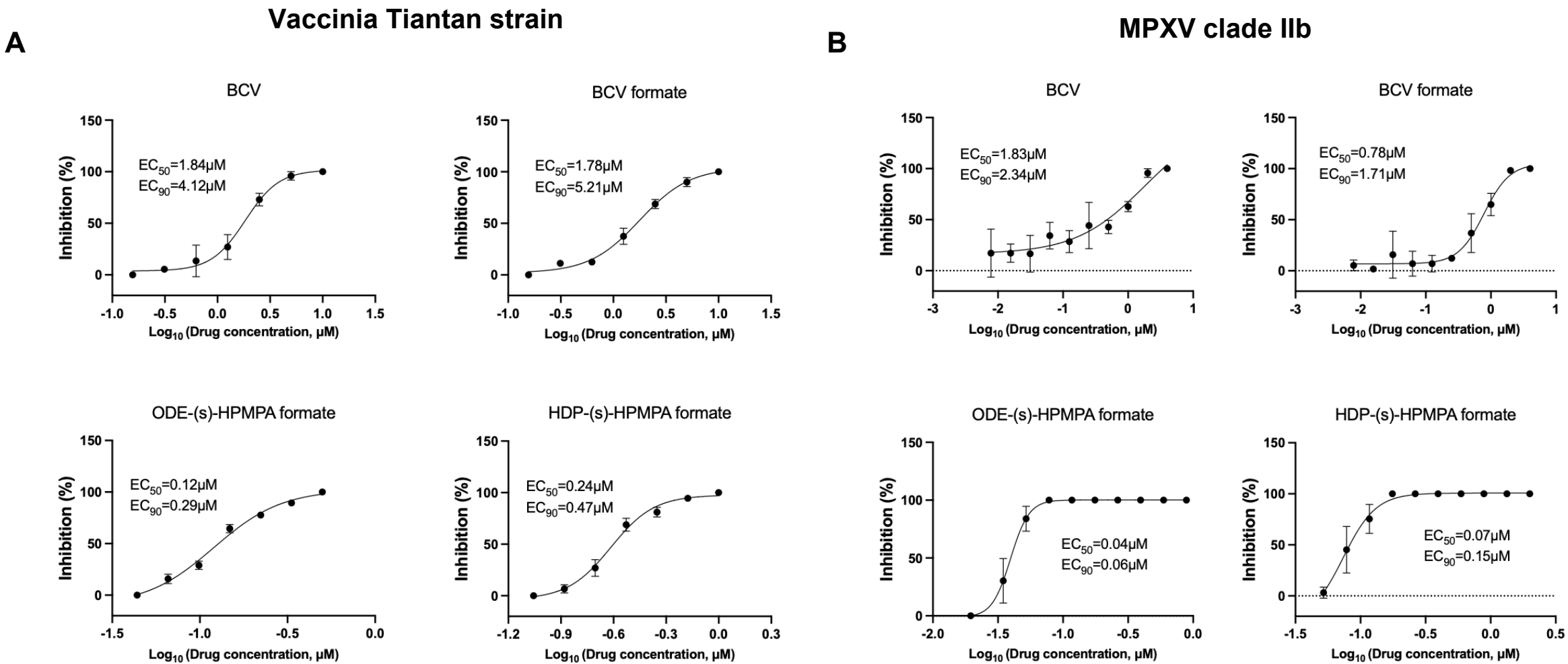
A
Vaccinia Tiantan strain
BCV
EC50=1.84μM
EC90=4.12μM
BCV formate
EC50=1.78μM
EC90=5.21μM
ODE-(s)-HPMPA formate
EC50=0.12μM
EC90=0.29μM
HDP-(s)-HPMPA formate
EC50=0.24μM
EC90=0.47μM
B
MPXV clade IIb
BCV
EC50=1.83μM
EC90=2.34μM
BCV formate
EC50=0.78μM
EC90=1.71μM
ODE-(s)-HPMPA formate
EC50=0.04μM
EC90=0.06μM
HDP-(s)-HPMPA formate
EC50=0.07μM
EC90=0.15μM
Inhibition (%)
Log10 (Drug concentration, μM)

Figure 4

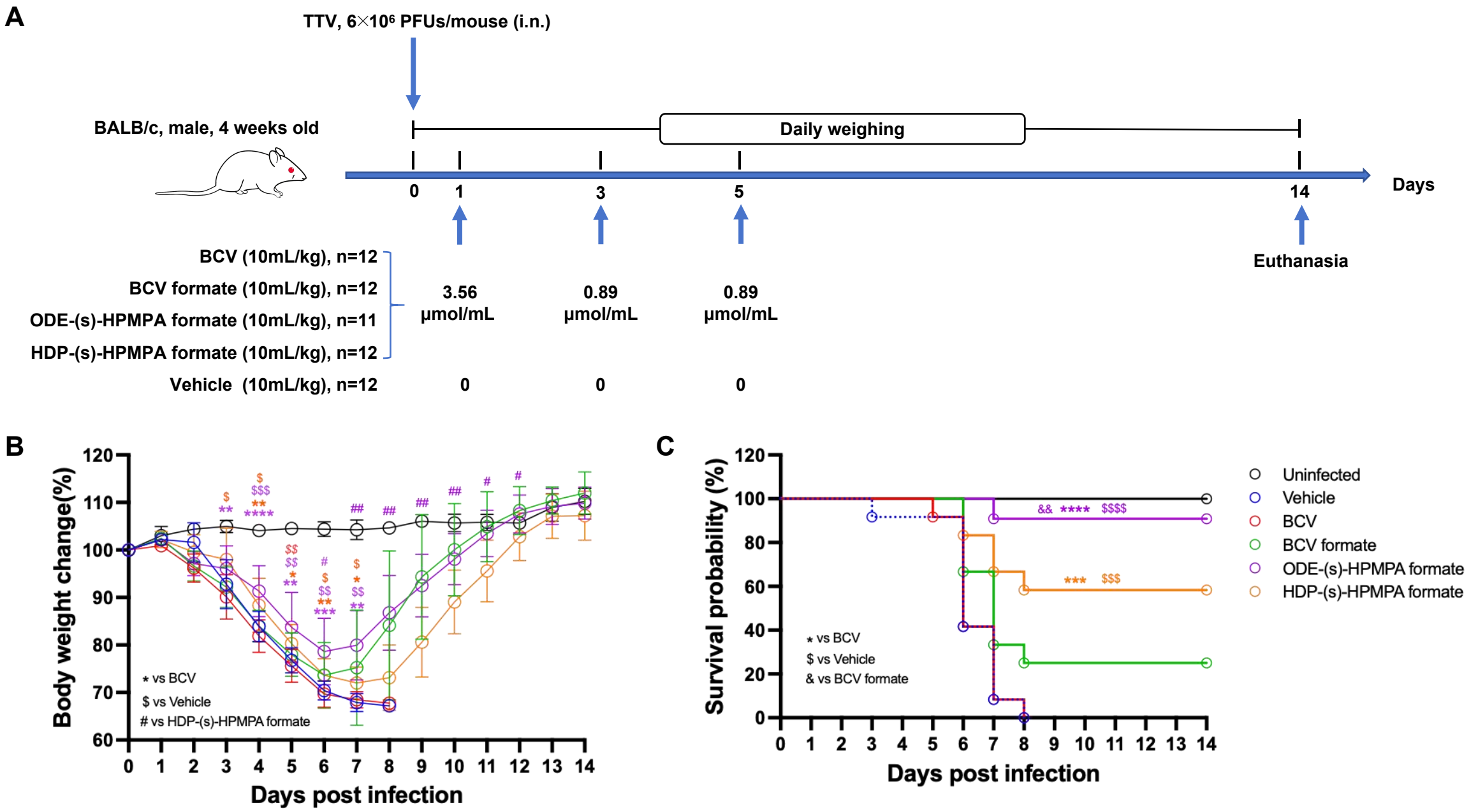
A
TTV, 6×10⁶ PFUs/mouse (i.n.)
BALB/c, male, 4 weeks old
Daily weighing
0
1
3
5
14
Days
Euthanasia
BCV (10mL/kg), n=12
BCV formate (10mL/kg), n=12
ODE-(s)-HPMPA formate (10mL/kg), n=11
HDP-(s)-HPMPA formate (10mL/kg), n=12
3.56 μmol/mL
0.89 μmol/mL
0.89 μmol/mL
Vehicle (10mL/kg), n=12
0
0
0
B
Body weight change(%)
Days post infection
* vs BCV
$ vs Vehicle
# vs HDP-(s)-HPMPA formate
C
Survival probability (%)
Days post infection
* vs BCV
$ vs Vehicle
& vs BCV formate
Uninfected
Vehicle
BCV
BCV formate
ODE-(s)-HPMPA formate
HDP-(s)-HPMPA formate

Figure 5

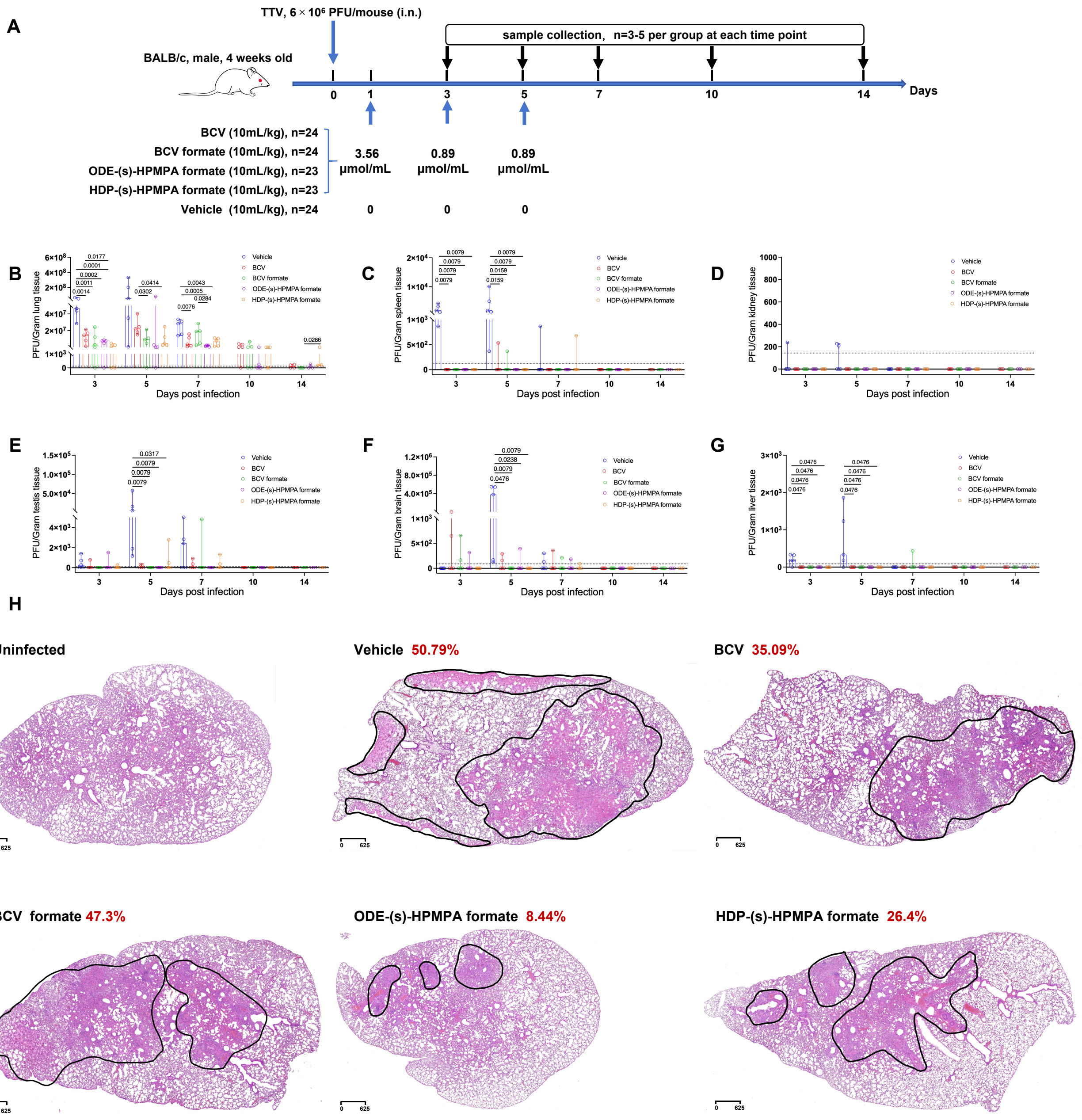
A
TTV, 6 × 10⁶ PFU/mouse (i.n.)
sample collection, n=3-5 per group at each time point
BALB/c, male, 4 weeks old
0
1
3
5
7
10
14
Days
BCV (10mL/kg), n=24
BCV formate (10mL/kg), n=24
ODE-(s)-HPMPA formate (10mL/kg), n=23
HDP-(s)-HPMPA formate (10mL/kg), n=23
3.56 μmol/mL
0.89 μmol/mL
0.89 μmol/mL
Vehicle (10mL/kg), n=24
0
0
0
B
PFU/Gram lung tissue
Days post infection
C
PFU/Gram spleen tissue
Days post infection
D
PFU/Gram kidney tissue
Days post infection
Vehicle
BCV
BCV formate
ODE-(s)-HPMPA formate
HDP-(s)-HPMPA formate
E
PFU/Gram testis tissue
Days post infection
F
PFU/Gram brain tissue
Days post infection
G
PFU/Gram liver tissue
Days post infection
H
Uninfected
Vehicle 50.79%
BCV 35.09%
BCV formate 47.3%
ODE-(s)-HPMPA formate 8.44%
HDP-(s)-HPMPA formate 26.4%
0
625

Figure 6

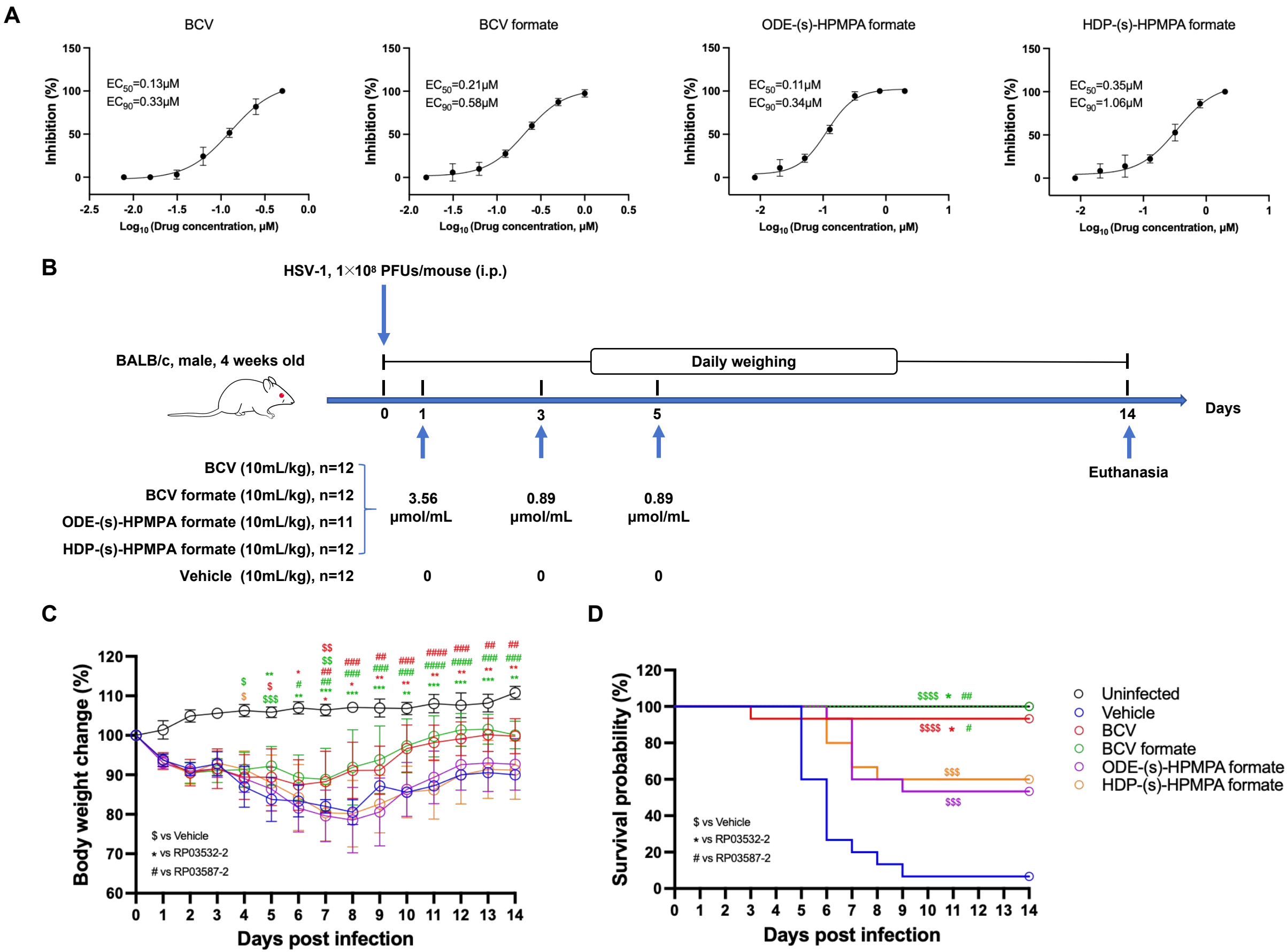
A
BCV
EC50=0.13μM
EC90=0.33μM
BCV formate
EC50=0.21μM
EC90=0.58μM
ODE-(s)-HPMPA formate
EC50=0.11μM
EC90=0.34μM
HDP-(s)-HPMPA formate
EC50=0.35μM
EC90=1.06μM
Inhibition (%)
Log10 (Drug concentration, μM)
B
HSV-1, 1×10⁸ PFUs/mouse (i.p.)
BALB/c, male, 4 weeks old
Daily weighing
Days
Euthanasia
BCV (10mL/kg), n=12
BCV formate (10mL/kg), n=12
ODE-(s)-HPMPA formate (10mL/kg), n=11
HDP-(s)-HPMPA formate (10mL/kg), n=12
3.56 μmol/mL
0.89 μmol/mL
0.89 μmol/mL
Vehicle (10mL/kg), n=12
0
0
0
C
Body weight change (%)
Days post infection
$ vs Vehicle
* vs RP03532-2
# vs RP03587-2
D
Survival probability (%)
Days post infection
Uninfected
Vehicle
BCV
BCV formate
ODE-(s)-HPMPA formate
HDP-(s)-HPMPA formate

Figure 7

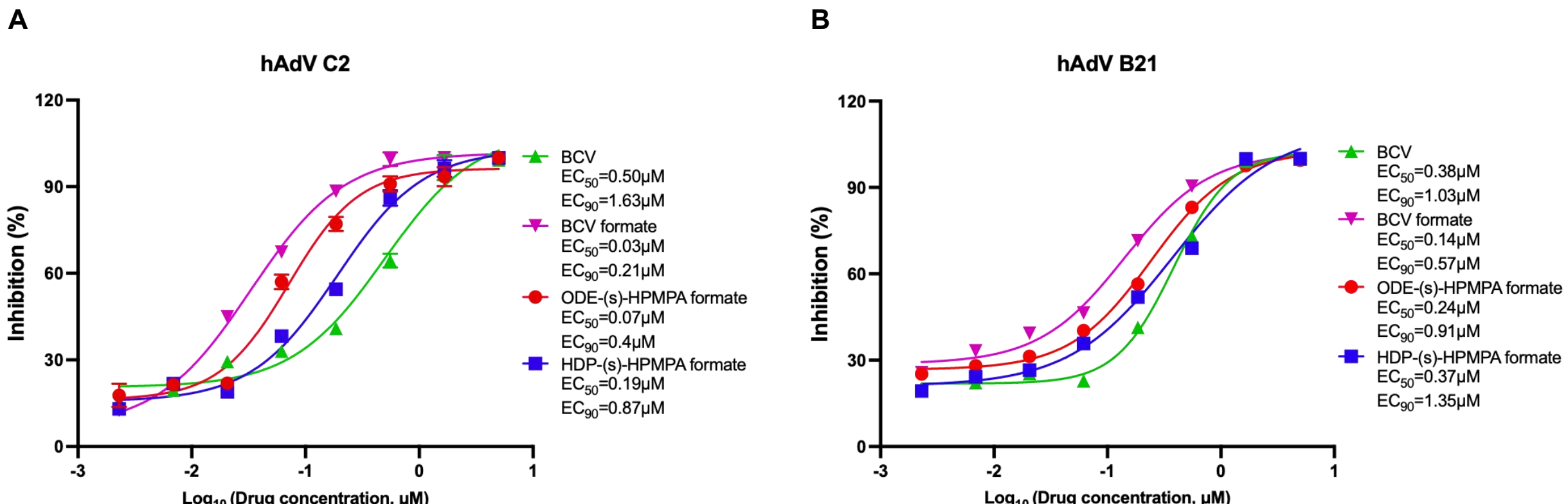
A
hAdV C2
Inhibition (%)
120
90
60
30
0
-3
-2
-1
0
1
Log10 (Drug concentration, μM)
BCV
EC50=0.50μM
EC90=1.63μM
BCV formate
EC50=0.03μM
EC90=0.21μM
ODE-(s)-HPMPA formate
EC50=0.07μM
EC90=0.4μM
HDP-(s)-HPMPA formate
EC50=0.19μM
EC90=0.87μM
B
hAdV B21
Inhibition (%)
120
90
60
30
0
-3
-2
-1
0
1
Log10 (Drug concentration, μM)
BCV
EC50=0.38μM
EC90=1.03μM
BCV formate
EC50=0.14μM
EC90=0.57μM
ODE-(s)-HPMPA formate
EC50=0.24μM
EC90=0.91μM
HDP-(s)-HPMPA formate
EC50=0.37μM
EC90=1.35μM